Chapter 5

Outcomes of cellular interactions between different AM colonization phenotypes with *rmc* tomato: insights into tomato plant responses blocking AM fungi

5.1. Introduction

The development of fungal structures in legume host plants to form a functional AM symbiosis involves at least three successive responses of different cell layers (Demchenko *et al.*, 2004; Novero *et al.*, 2002) and expression, even before contact, of different infection-related genes (Chabaud *et al.*, 2002; Weidmann *et al.*, 2004). Understanding part of this process in legumes has been possible due to the use of legume mutants, targeted first for being impaired in the nodulation process. However, most of terrestrial plants do not form rhizobial symbiosis and the utilization of *rmc* tomato to understand AM development in non legumes has been important.

The mutant *rmc* forms at least three phenotypes depending on the AM fungus that is colonizing (Pen-, Coi- and Myc+; Chapter 1, Section 1.3.2. for more details). After challenging *rmc* against many different AM fungi, Barker *et al.* (1998) and then Gao *et al.* (2001) showed that AM structures formed varied considerably. In Chapter 3, I found that *S. calospora* WUM 12(2) forming Coi- phenotype, and *G. intraradices* WFVAM23 forming Myc+ phenotype were colonizing *rmc* (no cortical colonization with *S. calospora*) to a high percentage. In a separate experiment (Chapter 6), I found that *G. intraradices* BEG159 heavily colonized the root surface of *rmc* and formed Pen- phenotype. Taking advantage of these different phenotypes, an experiment was designed with the general aim of characterizing cellular

modifications that occur in the different phenotypes of *rmc* during fungal colonization.

Gao *et al.* (2001) included quantification of colonization using the usual trypan blue staining method and laser scanning confocal microscopy (LSCM) to confirm the phenotypes. However, the cellular interactions of resistance to AM fungi by this mutant have not been investigated. Activation of plant defense responses which may provoke changes in autofluorescence and reinforcement of the host cell walls, including callose deposition, have been observed in failed interactions with mutant plants (Gianinazzi-Pearson *et al.*, 1991a; Gollotte *et al.*, 1993). A specific aim of the present work was to investigate whether similar plant defense reactions are induced in *rmc* tomato by AM fungi showing different phenotypes. In addition, activation of the root cells, including changes in the position of the nucleus of mutant plants, as well as activity, number and morphology of the fungal structures formed with *rmc* were also investigated.

5.2. Material and methods

5.2.1. Experimental settings and design

The AM fungi used in this experiment formed different phenotypes with *rmc*; Pen- with *G. intraradices* BEG159; Coi- with *S. calospora* WUM 12(2) and Myc+ with *G. intraradices* WFVAM23. Two nurse pots per fungus (one for wild-type and one for *rmc*) containing four tomato plants were used as experimental units and each plant in the same unit was considered a replicate. A non-inoculated control pot was included for each plant genotype. The nurse pots described by Rosewarne *et al*.

(1997) were used to obtain heavily colonized tomato plants. Briefly, two sterile seeds of *Trifolium subterraneum* L. cv. Mount Barker were planted in the middle of 1.4 kg pots containing a mix of either 10% Mallala or Kuitpo soil (depending on the fungal species, see Section 2.2) and 90% of sterile sand (3:1 coarse: fine sand). Inoculum of the fungi was incorporated as dry inoculum at a rate of 10% of the total soil weight; non-inoculated pots received 10% sterile soil-sand mix (Section 2.1). Nurse pots were grown for 8-12 weeks in a growth chamber under the same conditions described in Section 2.3. Half-strength Long Ashton solution (minus P) was applied every week at 10 mL kg soil^{-1} during the first 6 weeks after the clover seedlings emerged. After 6 weeks the amount was changed to 50 mL kg soil^{-1} until tomato plants were harvested. P as $CaHPO_4$ at 0.25 g kg^{-1} was incorporated directly into the soil mix before planting the nurse plants as described in Section 2.2.

Before transplanting tomatoes to the nurse pot, clover shoots were cut off to minimize competition between species. Tomato plants were harvested 3-21 days after planting. Wild-type tomato was harvested 3-4 days after planting in the nurse pots because they became rapidly colonized. Mutant plants were harvested 7-21 days after transplanting (depending on the fungal species) because colonization was always delayed. As wild-type and *rmc* plants were harvested at very different times, biomass was not determined in this experiment. Each plant was considered a replicate. Data from NBT/AF were analyzed as a two-way ANOVA in a completely randomized design from GENSTAT statistical software for Windows version 6 (Lawes Agricultural Trust, 2002). The differences among tomato plants with each fungus were established by one-way ANOVA and were considered significantly different when $P \leq 0.05$. Details of treatments are presented in Table 5.1.

Table 5.1. Experimental design used in this experiment including phenotypes with *rmc*.

Factor	Level	Phenotype with *rmc*
2 tomato genotypes	wild-type *rmc*	_
4 fungal treatments	*Glomus intraradices* BEG159 *Scutellospora calospora* WUM 12(2) *Glomus intraradices* WFVAM23 Non-mycorrhizal control	Pen- Coi- Myc+ _
1 harvest	8 pots with four plants in each	_

5.2.2. Harvesting and assessment of AM structures

Each pot was soaked in RO water for at least 30 minutes before harvesting to allow roots to be separated more easily from soil. Roots were washed out carefully with tap water and only those roots firmly attached to the plant were used for analysis of colonization. The root systems were very small and were separated into three parts. One fresh sample of approximately 0.8 g (fresh weight) was placed on a glass slide with 1:1 (v/v) glycerol:phosphate buffer (KH_2PO_4 and Na_2HPO_4, 0.05M, pH 7.4) and observed with a Nikon Eclipse TE300 inverted microscope coupled with UV filter set (excitation 340-380 nm wave length) to detect autofluorescence. Another sample of 0.8 g fresh weight was used for vital staining with nitroblue tetrazolium (NBT)/acid fuchsin (AF) (Section 2.7.1) to detect active and dead fungal structures. The remainder was fixed overnight in Carnoy's fluid (Section 2.5) at 4°C. The fixed sample was divided in three parts, one to be stained with DAPI (4',6'-diamino-2-phenylindole, Section 2.7.2) for assessment of plant and fungal nuclei, another with aniline blue for detection of callose deposition (Section 2.7.3). The third was stored

in 70% ethanol (v/v) to be used in case of failure of any of the stains mentioned before.

After staining with NBT/AF, roots were inspected under a dissecting microscope (10X, Olympus Sz11) and only colonized roots were mounted on a glass slide with 100% glycerol for examination of each mycorrhizal structure using the Bio-Rad multi-photon system (Nikon Eclipse TE300 inverted microscope) in light microscopy mode (Section 2.7.2). The method allowed detailed descriptions of dead fungal structures (bright pink) as well as active living structures (purple) (Smith and Dickson, 1991). To quantify mycorrhizal colonization, the classification described in Section 2.6 was used, but pink (dead) or purple (alive) structures were recorded separately.

The roots fixed in Carnoy's fluid were re-hydrated by placing them for 30 minutes in 70% ethanol (v/v), 30 minutes in 30% ethanol, and 20 minutes in RO water (twice). One part of the roots was then treated overnight with DAPI (Section 2.7.2), mounted on glass slides and examined under the Bio-Rad multi-photon system (Nikon Eclipse TE300 inverted microscope coupled with Coherent Mira900-F titanium:saphire ultra-fast laser) with UV excitation/emission at 358/461 nm. Several series of xy-slices with an interval of 0.5-1.0 μm in the z-axis were collected for both wild-type and *rmc* tomato root cells. The images were collected and merged using CAS imaging software (Confocal Assistant System, Copyright © 1994; Todd Clark Brelje, Bio-Rad).

The other sample of re-hydrated roots was embedded in LR white resin (O'Brien & McCully, 1981) and 5 μm transverse sections were stained with AB (Section 2.7.3). Bright yellow fluorescence, detected with a Leica SP5 spectral scanning confocal

microscope with UV and blue excitation/emission wavelengths of 370/509 nm, was taken as the indication of callose deposits. A 3D visualization using a GMA filter was also performed to localize fungal tissue more easily. Images were collected using Leica Application Suit AF (LAS Leica, Japan).

5.3. Results

5.3.1. AM mycorrhizal structures with the wild-type tomato

Three days after being transplanted in the nurse pots, the three fungi formed all types of mycorrhizal structures with the wild-type including vesicles.

5.3.1.1. Active and dead fungal structures. *G. intraradices* BEG159 formed elongated appressoria (Appr) before penetrating the epidermal cells (Figure 5.1a and 5.1b). Intraradical hyphae (IH) grew from cell to cell until reaching the outer cortical cells (Figure 5.1c). Dichotomously branched and terminal arbuscules were formed in the cortex and IH grew to the next cell through the intercellular spaces (Figure 5.1d), typical of an *Arum*-type mycorrhiza. Data showed that up to 86.4% of fungal structures were active, indicated by the NBT/AF stain (Table 5.2, page 103).

S. calospora WUM 12(2) penetrated the epidermis directly, without appearing to form any appressorium (Figure 5.2a). IH grew from cell to cell until reaching the cortex and then formed intracellular hyphal coils and arbusculate coils (Figure 5.2b and 5.2c). Sometimes after forming arbusculate coils, IH grew to the next cell using the intercellular spaces, which placed the AM type as intermediate 4 (I4). Between 70% and 80% of all fungal structures were active (Table 5.2, page 103).

G. *intraradices* WFVAM23 formed globe-like appressoria on the root surface before becoming intraradical (Figure 5.3a). It formed a typical *Arum*-type AM with terminal finely branched arbuscules. IH grew through the intercellular spaces (Figure 5.3b and 5.3c). Up to 92% of these IH were active with the wild-type (Table 5.2, page 103).

5.3.1.2. Position of wild-type plant nuclei in root cells. Staining roots with DAPI allowed detection of the position of the plant nuclei in root cells and visualization of fungal nuclei in the hyphae (Figure 5.4a). Confocal microscopy clearly showed the entry points containing clusters of fungal nuclei (Figure 5.4b). After IH penetrated cortical cells, movement of the plant nuclei to the middle of the cell occurred and did not vary between fungal species. The plant nucleus was surrounded by the hyphal branches of arbuscules or arbusculate coils (Figures 5.4c and 5.4d).

5.3.1.3. Autofluorescence and detection of callose deposition. Autofluorescence observed under UV and blue light excitation was localized around fungal hyphae at the penetration points on the root surface or where hyphae grew from cell to cell in the wild-type (Figure 5.5a and 5.5b). This autofluorescence was not detected when fully developed arbuscules were seen in cortical cells of the wild-type. Deposits of callose were occasionally detected in cortical cells containing IH and arbuscules and/or arbusculate coils, but not at entry points. These deposits were very small and rarely seen (Figure 5.5c, 5.5d, 5.5e and 5.5f). Figure 5.5 is presented on page 100 and its caption on page 101.

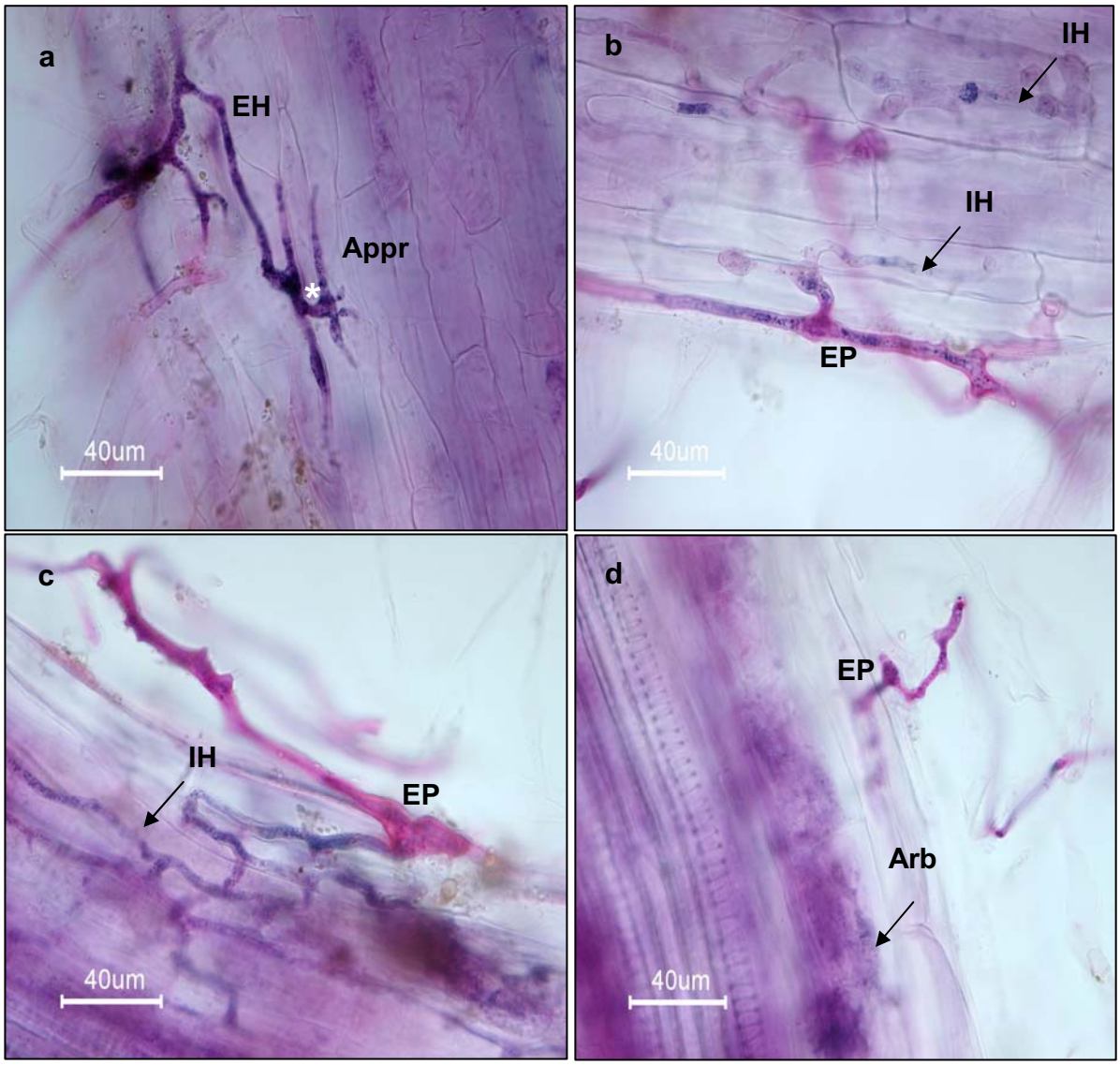

Figure 5.1. Wild-type tomato roots colonized with *G. intraradices* BEG159 and stained with NBT/AF to detect active and dead fungal structures. a) Active and elongated appressorium (Appr *); b and c) Intraradical hyphae (IH) growing from cell to cell (arrowed) until reaching the outer cortical cells; d) dichotomously branched and terminal arbuscules (Arb, arrow) typical of *Arum*-type mycorrhizas. EH, external hyphae; EP, entry point. Resolution is better on CD provided in this thesis, see file “figure_5_1”.

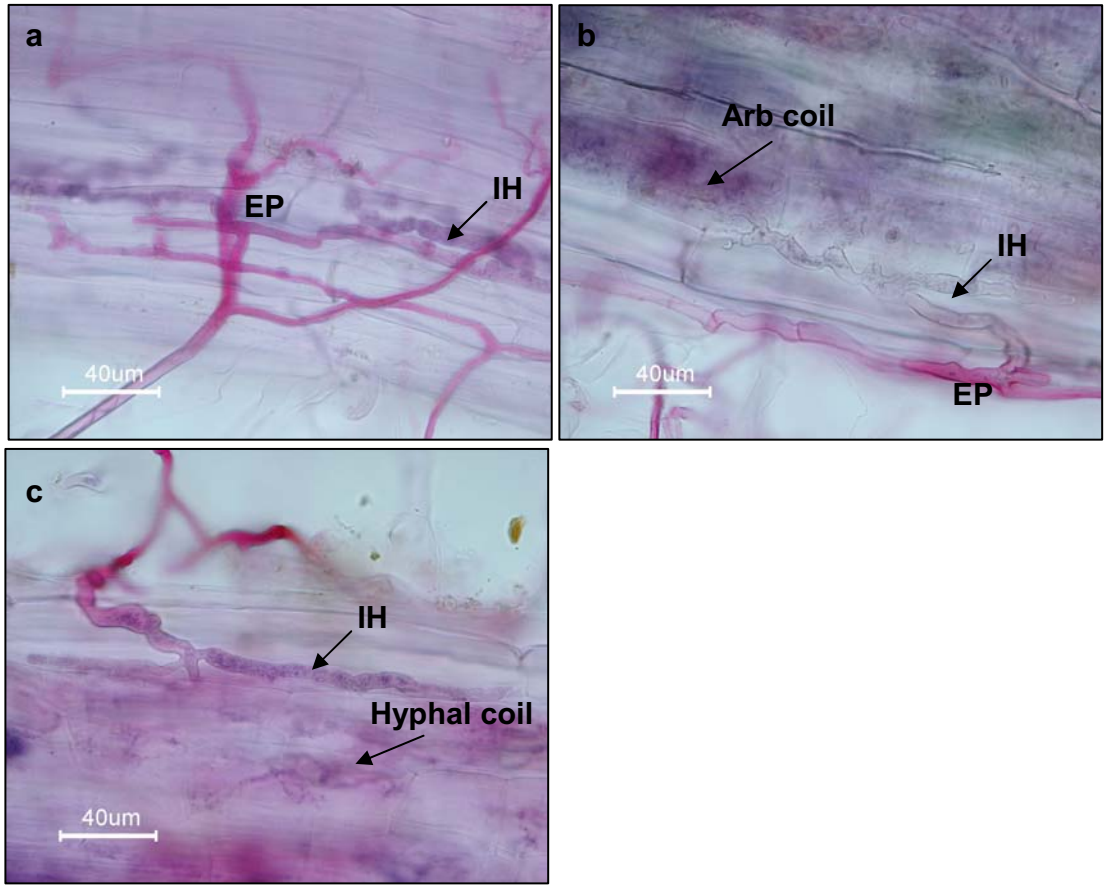

Figure 5.2. Wild-type tomato roots colonized with *S. calospora* WUM 12(2) and stained with NBT/AF to detect active and dead fungal structures. a) Entry point (EP) without visible appressorium and arrow showing internal hyphae (IH) growing from cell to cell. b) Intraradical hyphae (IH) formed arbusculate coils (arrow) or c) hyphal coils (arrow) in cortical cells. Resolution is better on CD provided in this thesis, see file “figure_5_2”.

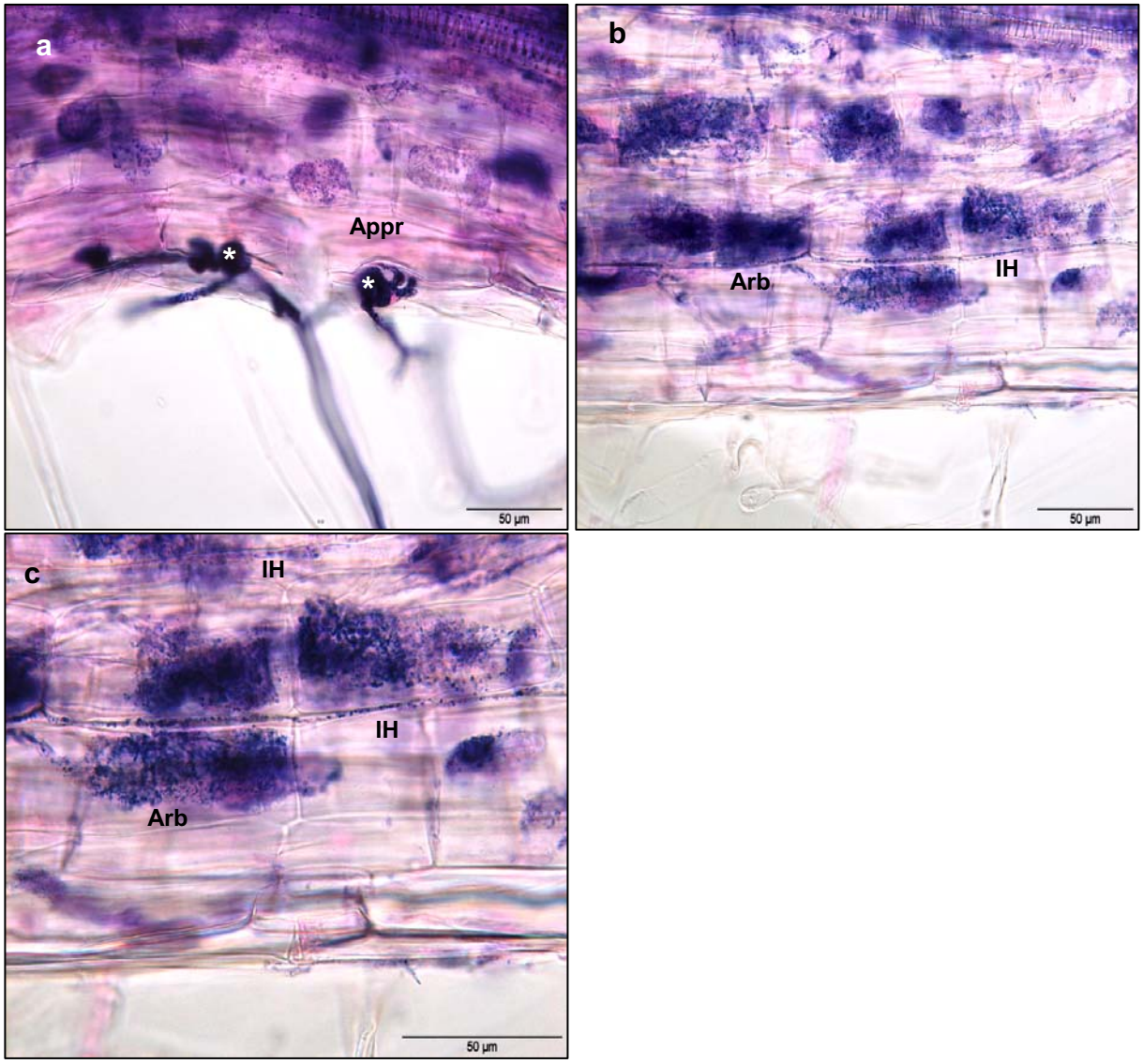

Figure 5.3. Wild-type tomato roots colonized with *G. intraradices* WFVAM23 and stained with NBT/AF to detect active and dead fungal structures. a) Active, globe-like and branched appressorium (Appr *); b and c) typical *Arum*-type arbuscules (Arb) and intraradical hyphae (IH) spreading by intercellular spaces. Arbuscules are dichotomously branched and terminal. Resolution is better on CD provided in this thesis, see file “figure_5_3”.

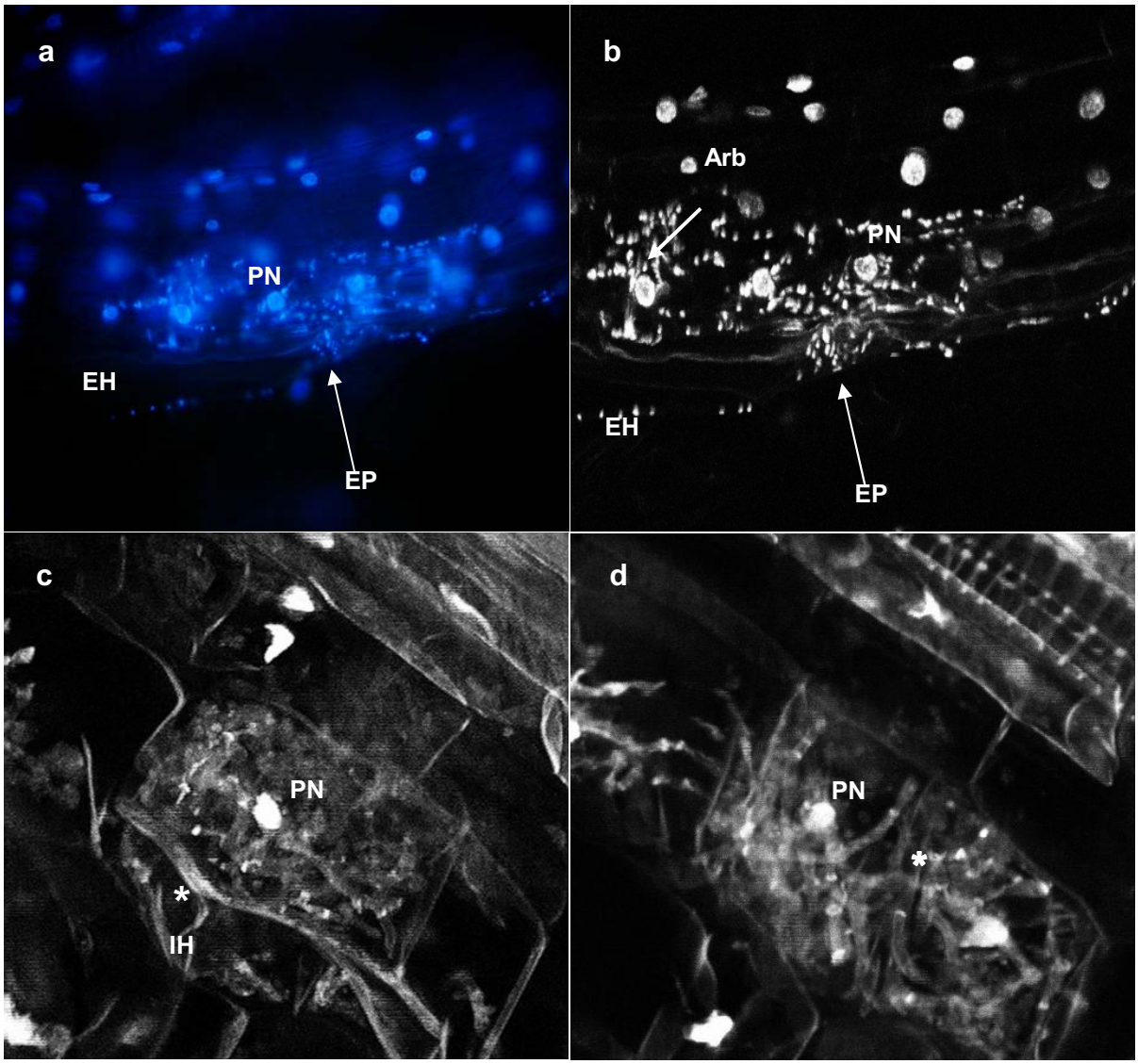

Figure 5.4. Roots of wild-type tomato stained with DAPI. a) UV-Fluorescence showing location of plant nuclei in the middle of the root cells when *G. intraradices* BEG159 was inoculated. b, c and d) LSCM extended focus images showing b) plant nuclei localized centrally in cells after arbuscules formation (Arb). Arrows showing fungal nuclei; c) details of a typical arbuscule formed with *G. intraradices* BEG159. Note the IH (*) from which arbuscules originated. d) Details of an arbusculate coil formed with *S. calospora* WUM(2). IH grew from cell to cell (*) to form new arbuscules. Resolution is better on CD provided in this thesis, see file "figure_5_4.ppt".

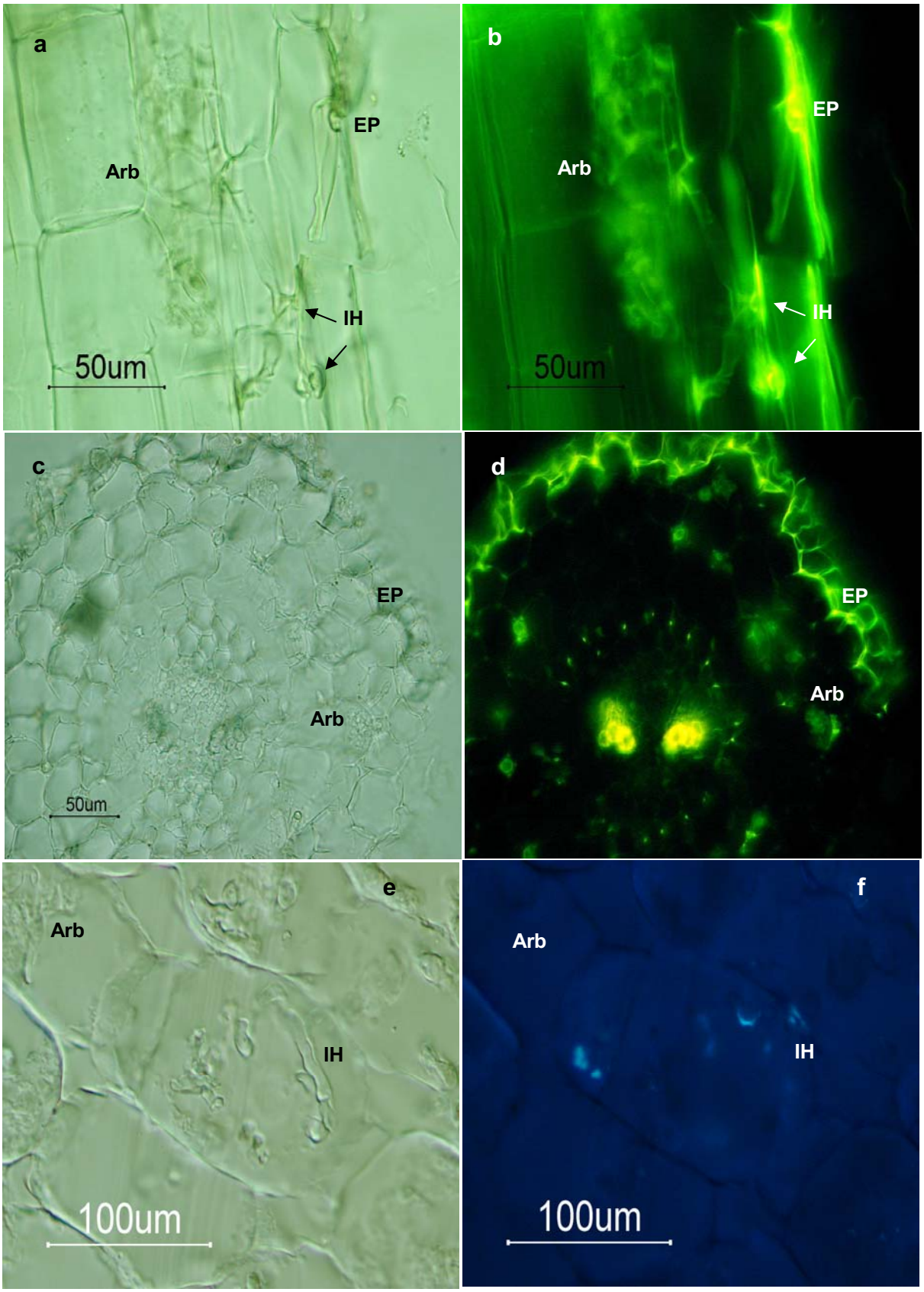
a
EP
Arb
IH
50um
b
EP
Arb
IH
50um
c
EP
Arb
50um
d
EP
Arb
e
Arb
IH
100um
f
Arb
IH
100um

Caption for Figure 5.5. Autofluorescence and callose deposition observed in wild-type tomato roots under bright field microscopy (a, c, e) and blue light excitation (b, d, f) of the same sections. a) and b) autofluorescence increased at the entry point (EP) and when internal hyphae (IH) grew from cell to cell when *G*. *intraradices* BEG159 was inoculated. c) and d) Callose detected with AB when *G*. *intraradices* BEG159 was inoculated was rarely observed. e) and f) Callose deposits in arbusculate (Arb) coils formed by *S*. *calospora* WUM 12 (2) were also uncommon. Resolution is better on CD provided in this thesis, see file "figure_5_5.ppt".

5.3.2. AM mycorrhizal structures with the mutant

Fungal development with *rmc* mostly included external hyphae (EH) in the Pen- phenotype. However, there were no significant differences when compared with the wild-type for either EH or number of appressoria. In the Coi- phenotype, reduced development of IH was observed. The percentage IH was significantly lower with *rmc*. In the Myc+ phenotype, the percentage of EH, IH and arbuscules were significantly lower when compared with the wild-type. Generally, around 50% of appressoria and entry points were found to be active in this genotype (Table 5.2). Although the percentages of IH in the Coi- and Myc+ phenotypes were reduced compared with the wild-type, almost 50% of them were active. All arbuscules in the Myc+ phenotype were active.

5.3.2.1. Characterization of active and dead fungal structures. In the Pen- phenotype with *G*. *intraradices* BEG159 active elongated appressoria very similar to those with the wild-type were formed (Figure 5.6a). These appressoria became highly branched when penetration failed (Figure 5.6b). If penetration did not occur, frequent cross walls were observed separating active from dead sections of EH (Figure 5.6c. and 5.6d). This pattern of development made *rmc* root surface look

bright pink because around 40% EH and appressoria were dead (Table 5.2). Occasionally, IH were found to penetrate and form arbuscules.

In the Coi- phenotype with *S. calospora* WUM 12(2), well-defined appressoria were not observed, but the EH attempting to penetrate the roots looked swollen and slightly branched (Figure 5.7a and 5.7b). If penetration failed, fungal hyphae formed cross walls that separated the dead appressoria and grew parallel to the root. New penetration attempts were observed next to the failed point (Figure 5.7c). When the penetration was successful, IH development was confined to one or two adjacent cells (Figure 5.7d) in the exodermis. These IH formed small, thick branches of which around 50% were dead. Cross walls were also observed separating active parts of IH from dead segments (Figure 5.7d).

The Myc+ phenotype with *G. intraradices* WFVAM23 formed balloon-like appressoria (Figure 5.8a), in addition to enlarged and branched ones (Figure 5.8b). However, both types were similar to those formed with the wild-type. Frequently these appressoria were dead (around 50%) and cross walls were formed in the fungal hyphae that separated the dead and active parts. Immediately adjacent to the dead appressoria, other attempts to penetrate were observed. Sometimes fungal hyphae penetrated and were restricted to the exodermis. These IH were mostly active (around 60%), thicker than the IH with the wild-type and did not reach the cortex (Figure 5.8c). However, if IH reached the cortex, they always formed arbuscules. These arbuscules were active and typical of the *Arum*-type with dichotomous and finely branched hyphae (Figure 5.8d) although reduced in number when compared with the wild-type (Table 5.2).

Table 5.2. Percentage root length colonized by different structures in wild-type and *rmc* tomato when inoculated with AM fungi forming different phenotypes. For each AM fungal species, means followed by the same letter in each category were not significantly different (P≤0.05) when the wild-type and *rmc* tomato were compared. Numbers in brackets are the percentages of these structures that were active in each category. These data are also used in Chapter 6. Labels are: Appr, appressoria; EH, external hyphae; IH, internal hyphae; Arb, arbuscules. *G. intraradices* BEG159 and *G. intraradices* WFVAM23 formed *Arum*-type AM. *S. calospora* formed Intermediate 4 (I4) type.

Fungal species	Appr		EH		IH		Arb	
	Wild-type	Mutant	Wild-type	Mutant	Wild-type	Mutant	Wild-type	Mutant
1 G. intraradices BEG159	12.1a(**70.7**)	8.7a(**57.1**)	57.5a(**60.7**)	76.1a(**60.6**)	65.7a(**75.2**)	6.7b(**100**)	61.8a(**86.4**)	5.0b(**100**)
S. calospora WUM 12(2)	37.3a(**70.3**)	41.8a(**64.8**)	69.4a(**67.8**)	57.8a(**51.3**)	58.1a(**80.7**)	16.3b(**49.9**)	55.2a(**79.9**)	0.0b
G. intraradices WFVAM23	24.7a(**61.5**)	53.1a(**48.4**)	44.4b(**56.**4)	94.3a(**43.1**)	93.3a(**87.**4)	29.0b(**56.5**)	79.6a(**92.0**)	11.5b(**100**)

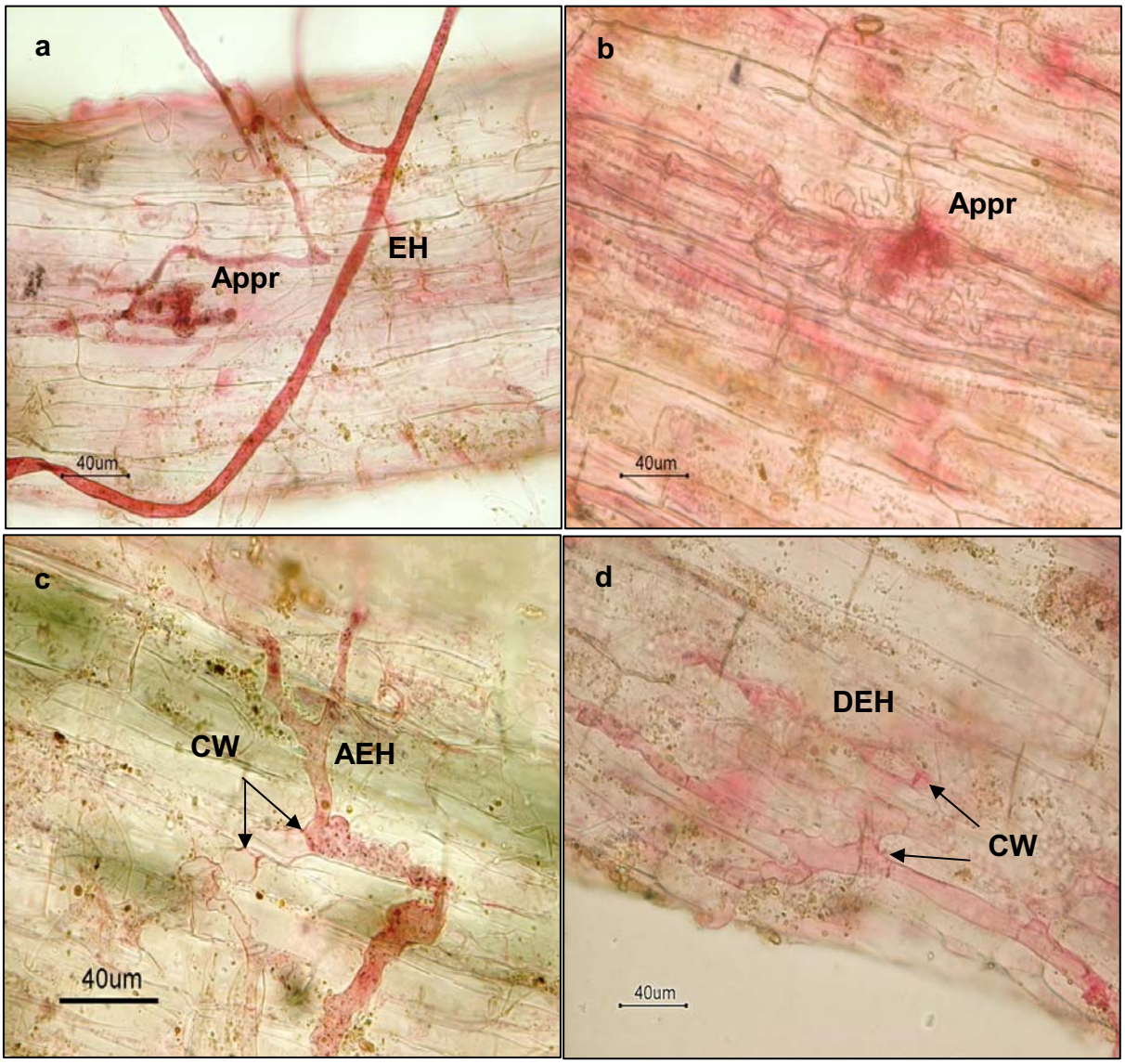

Figure 5.6. Roots of *rmc* tomato colonized by *G. intraradices* BEG159 and stained with NBT/AF to detect active and dead fungal structures. a) Active, normal appressorium (Appr). b) Dead and highly branched appressoria. c) Cross walls (CW) separating active (AEH) from dead EH (DEH). d) Root surface with DEH in which CW can be observed. Resolution is better on CD provided in this thesis, see file "figure_5_6.ppt".

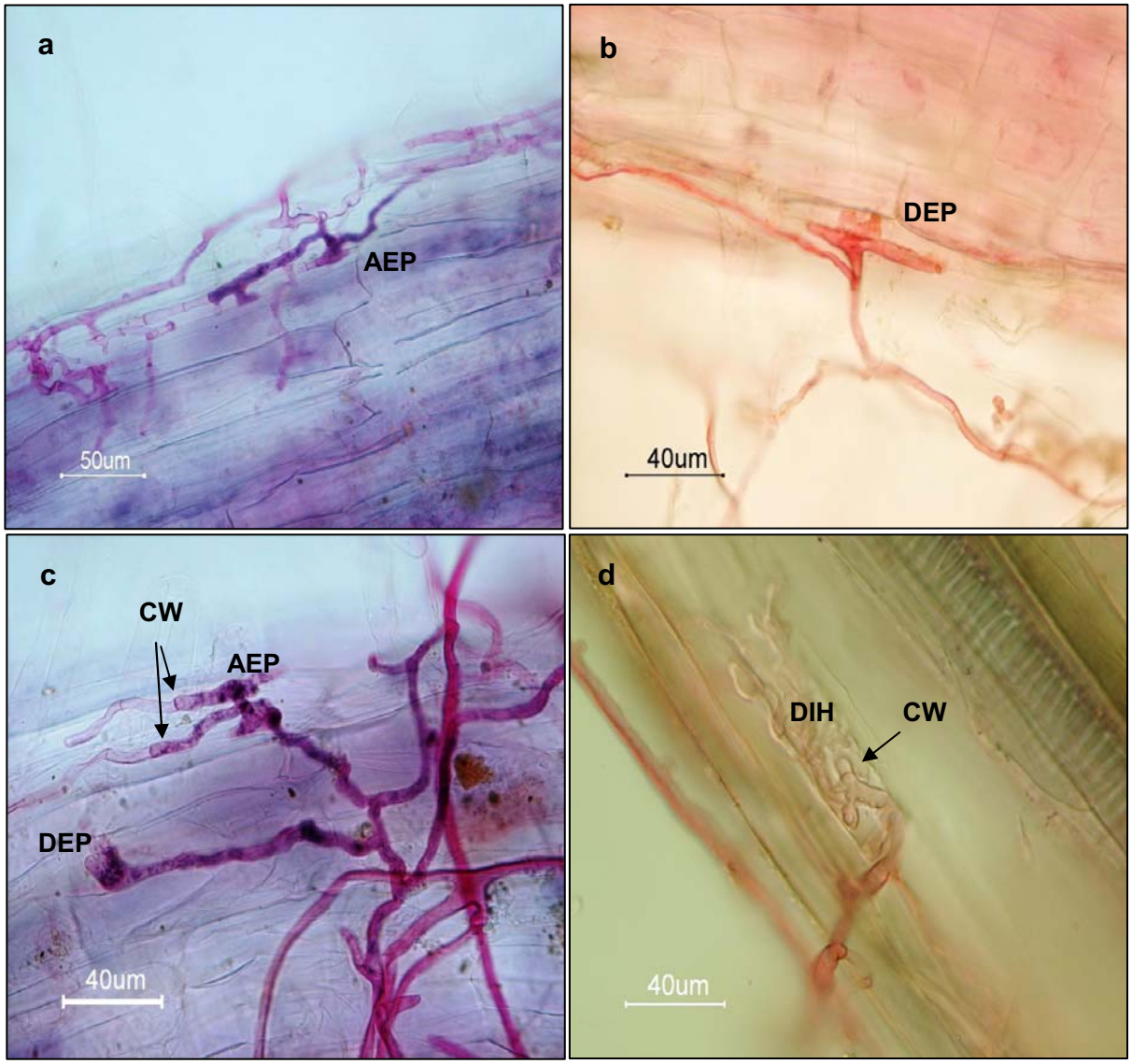

Figure 5.7. Roots of *rmc* tomato colonized by *S. calospora* WUM 12(2) forming Coi-phenotype. Root segments were stained with NBT/AF to detect active and dead fungal structures. a) Active entry point (AEP). b) Dead swollen and slightly branched EP. c) Cross walls (CW) separating active (AEP) from dead entry points (DEP) after failing penetration. d) Dead internal hyphae (DIH) blocked at the exodermis, showing thick branches and CW. Resolution is better on CD provided in this thesis, see file “figure_5_7.ppt”.

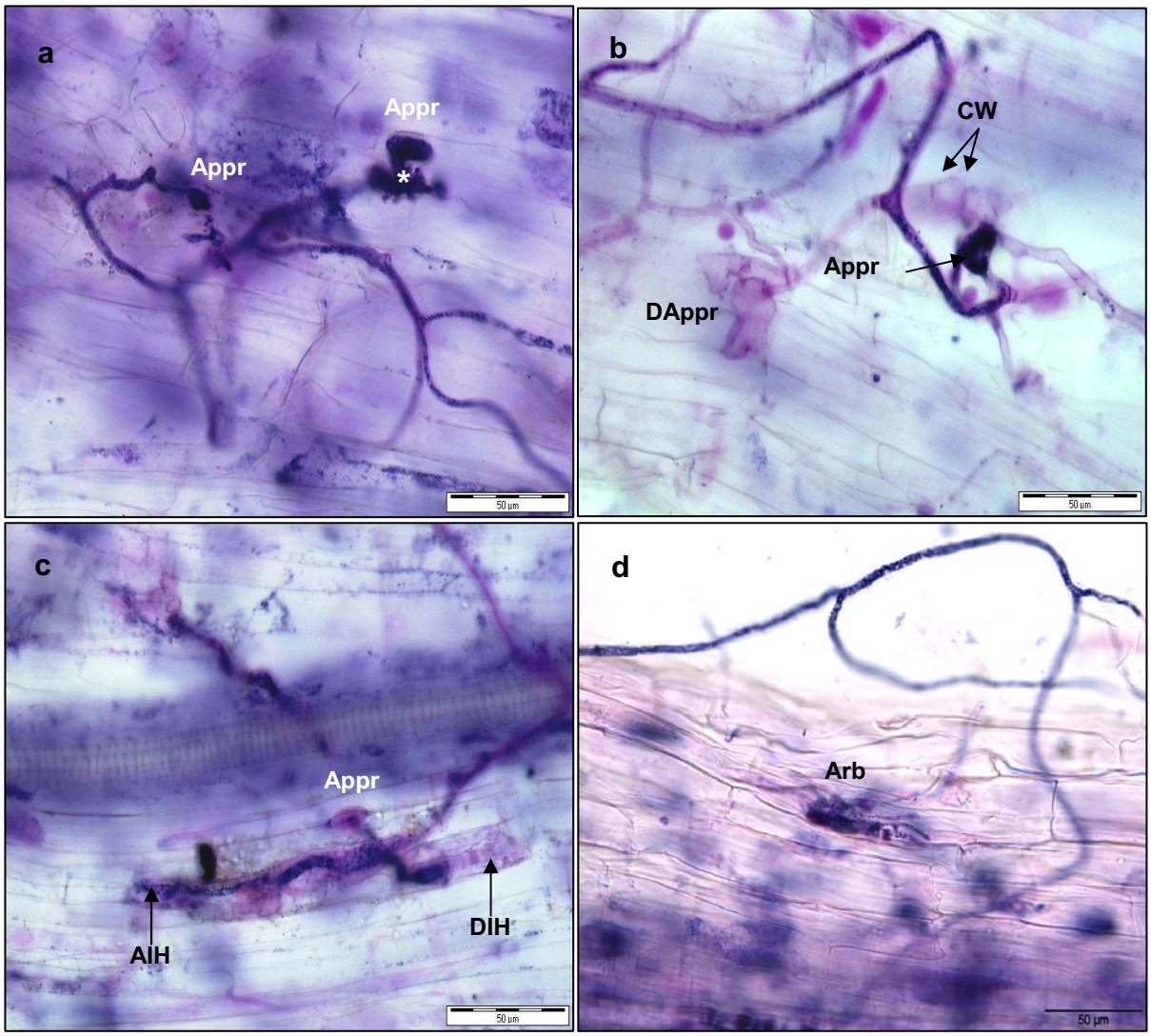

Figure 5.8. Roots of *rmc* tomato colonized by *G. intraradices* WFVAM23, forming Myc+ phenotype. Root segments were stained with NBT/AF to detect active and dead fungal structures. a) Active, balloon-like appressorium and branched appressorium (*). b) Dead (DAppr) and active swollen appressoria (Appr); this picture also shows cross walls (CW) in dead appressorium. c) Active (AIH) and dead (DIH) internal hyphae after penetration. d) Active arbuscules (Arb) typical of *Arum*-type AM. Resolution is better on CD provided in this thesis, see file "figure_5_8.ppt".

5.3.2.2. Position of mutant plant nuclei. DAPI clearly stained *rmc* and fungal nuclei in whole root segments. In the Pen- phenotype with *G. intraradices* BEG159 the position of plant nuclei did not change in response to the formation of fungal appressoria. Each of these appressoria contained several nuclei (Figure 5.9a), the presence of which was confirmed with confocal microscopy (Figure 5.9b). Fungal nuclei disappeared when the penetration failed and cross wall formation was observed (Figure 5.9c and 5.9d).

In the Coi- phenotype with *S. calospora* WUM 12(2), the presence of appressoria on the root surface of *rmc* was not followed by movement of plant nuclei (Figure 5.10a). However, when hyphae became intraradical, plant nuclei moved slightly from its original position, towards a central position in exodermal cells (Figures 5.10b, 5.10c and 5.10d). IH in the exodermis did not proceed further to the cortex to form arbuscules, and cross walls were formed in the fungal hyphae. The nuclei of cortical cells remained at the periphery of the cells, as occurred before the penetration.

In the Myc+ phenotype with *G. intraradices* WFVAM23, the position of nuclei of *rmc* tomato was not altered either by presence of appressoria on the root epidermis (Figure 5.11a) or by failed colonization in the exodermis (Figures 5.11b and 5.11c). However, when the fungus reached the cortex and formed arbuscules, the *rmc* cell nucleus was observed in a central position similar to the wild-type (Figure 5.11d).

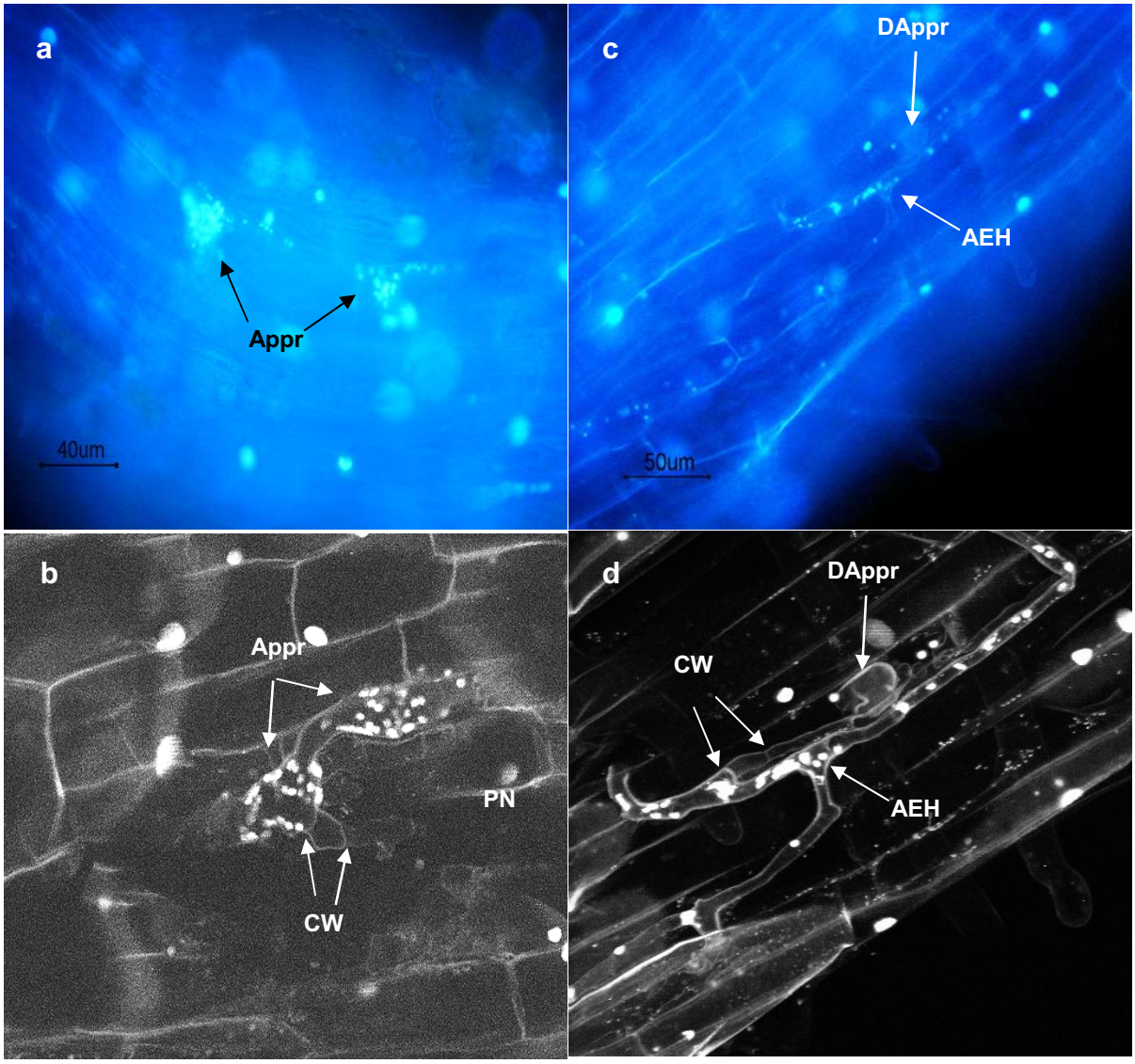

Figure 5.9. Pen- phenotype in *rmc* with *G. intraradices* BEG159. Roots were stained with DAPI. UV Fluorescence (a, b) and LSCM extended focus images (c, d); a) and d) active appressoria (Appr) are seen as clusters of fungal nuclei, which were confirmed with confocal microscopy. r*mc* plant nucleus stayed at the periphery of the cell when appressoria were active. b) and d) Dead appressorium (DAppr) did not contain nuclei. Using confocal imaging, cross walls were observed separating active EH from dead EH on epidermal cells. PN, plant nuclei; CW, cross walls; AEH, active external hyphae. Resolution is better on CD provided in this thesis, see file "figure_5_9.ppt".

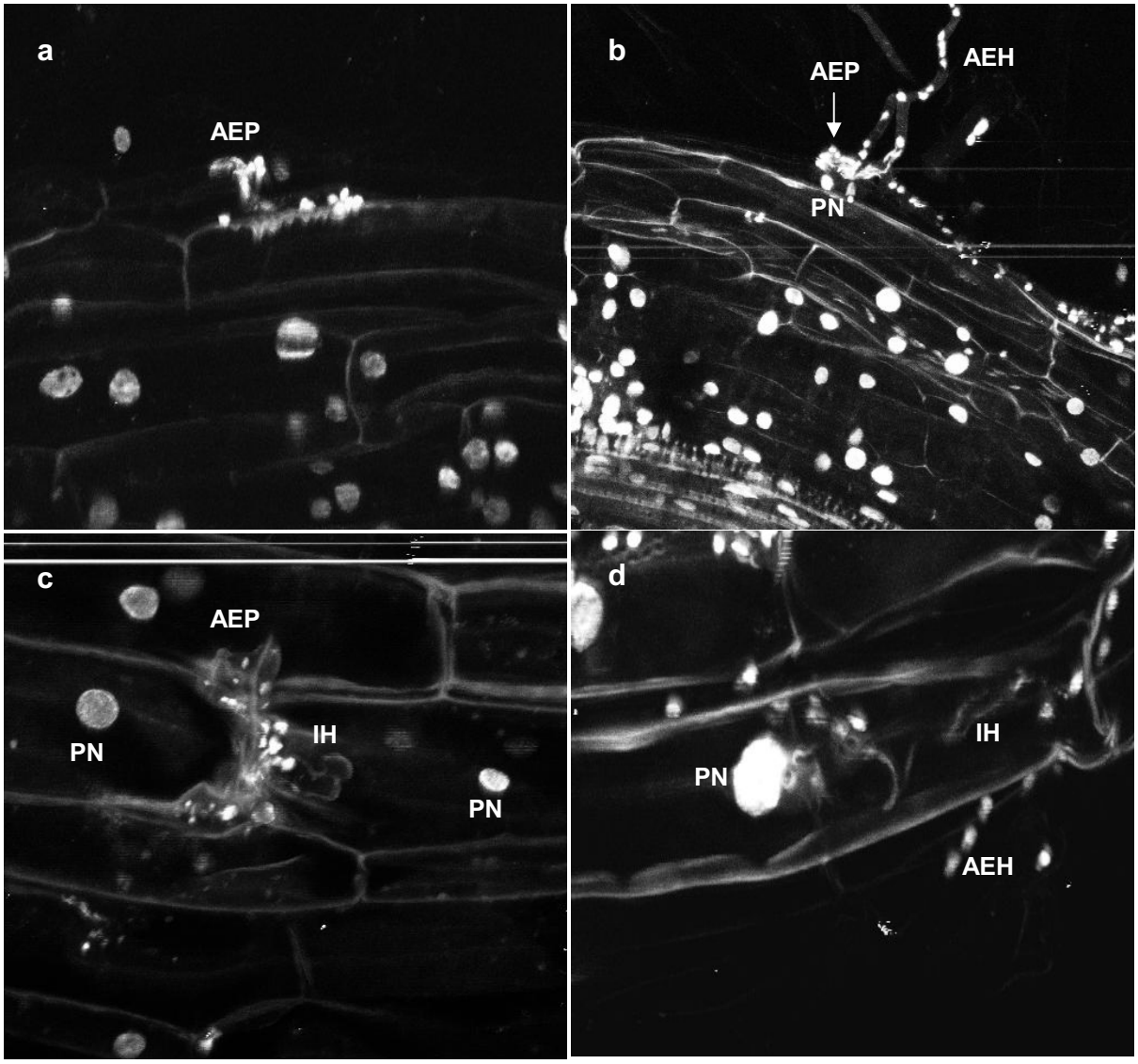

Figure 5.10. LSCM extended focus images of the Coi- phenotype in *rmc* with *S. calospora* WUM 12(2). Roots were stained with DAPI. a) Active entry point (AEP) on the surface of an epidermal cell showing fungal nuclei. b, c and d) After fungal penetration of epidermal and exodermal cells, the position of *rmc* nuclei changed to a central position. AEH, active external hyphae; PN, plant nuclei; IH, internal hyphae. Resolution is better on CD provided in this thesis, see file "figure_5_10.ppt".

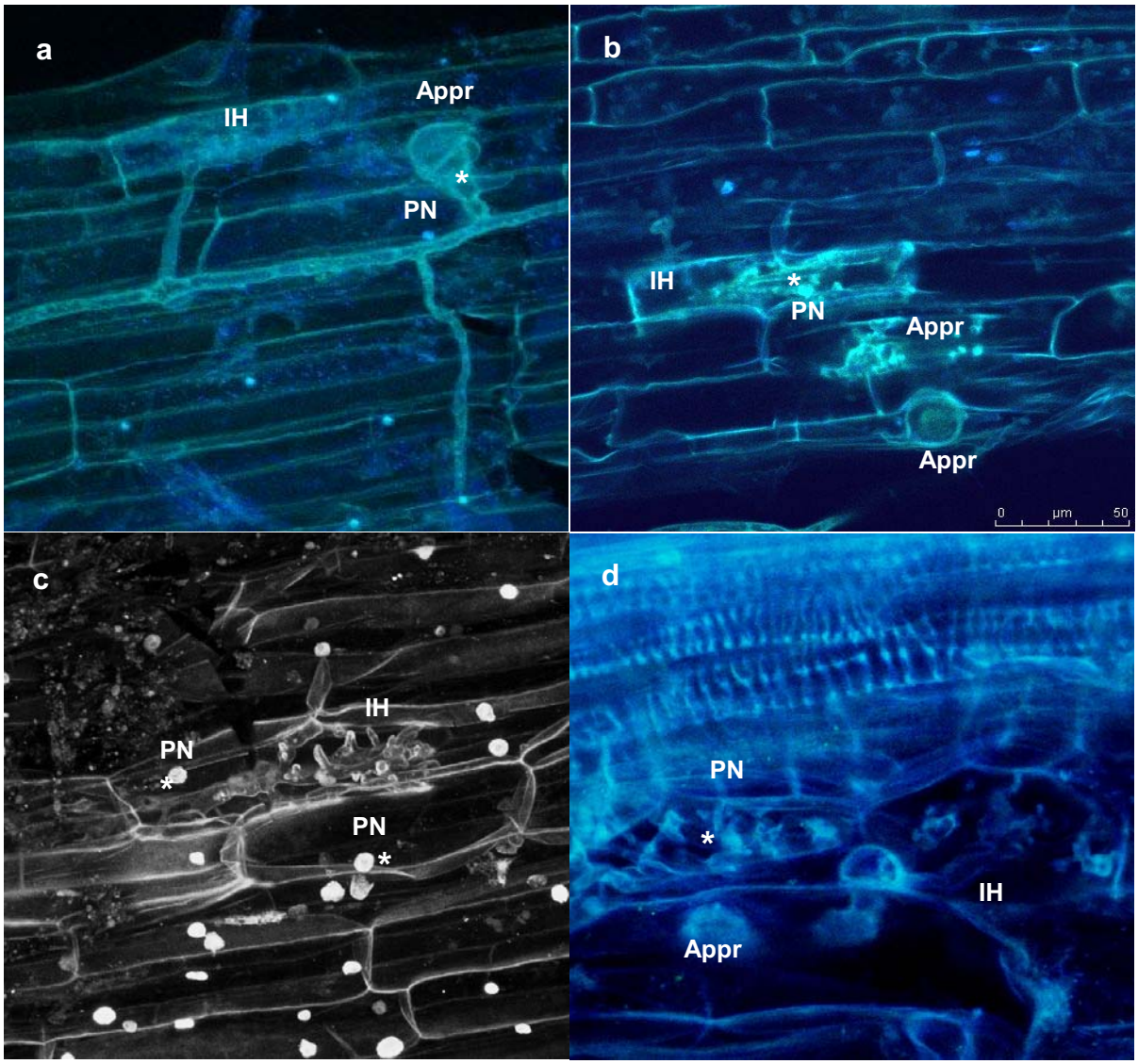

Figure 5.11. LSCM extended focus images of the Myc+ phenotype in *rmc* with *G. intraradices* WFVAM23. Roots were stained with DAPI. a) Balloon-like appressorium with a hyphal branch (*), the PN is at the periphery of the cell. b) After penetration of the exodermis, IH reached the cortical cells. The nuclei of *rmc* can be seen to have moved to a central position. c) When IH growth was blocked, *rmc* nuclei were seen at the periphery of the cell. d) Typical *Arum*-type arbuscules were formed with the plant nucleus surrounded by the fungal hyphal. PN, plant nuclei; IH, internal hyphae; Appr, appressorium. Resolution is better on CD provided in this thesis, see file “figure_5_11.ppt”.

5.3.2.3. Autofluorescence and detection of callose deposition. Independent of the mycorrhizal phenotype, autofluorescence was observed at the points of appressorium formation. This fluorescence developed all along EP (encapsulating the appressorium, Figure 5.12a and 5.12b) and in the IH, after penetration of the epidermis (Figure 5.12c). This was not observed when appressoria were dead (presence of cross walls, Figure 5.12d) or when arbuscules were completely developed. Deposits of callose were not detected at the EP or IH with any of the phenotypes (Figure 5.12e and 5.12f).

Caption for Figure 5.12. Autofluorescence (a, b, c, d) and aniline blue staining for detection of callose deposition (e, f) in *rmc* tomato. Autofluorescence was observed in a) and b) encapsulating appressoria before penetration of epidermal cells when *G. intraradices* WFVAM23 was inoculated, and c) around IH after penetration of the epidermis. d) No autofluorescence was detected at the point of contact of dead appressorium of *G. intraradices* BEG159. e) Bright field light microscope image showing *S. calospora* hyphae after penetration of the epidermis and f) the same field observed with UV light to detect callose. Deposits of callose were not detected in any of the phenotypes. Appr, appressorium; IH, internal hyphae; DAppr, dead appressorium Resolution is better on CD provided in this thesis, see file "figure_5_12.ppt". Figure appears on next page.

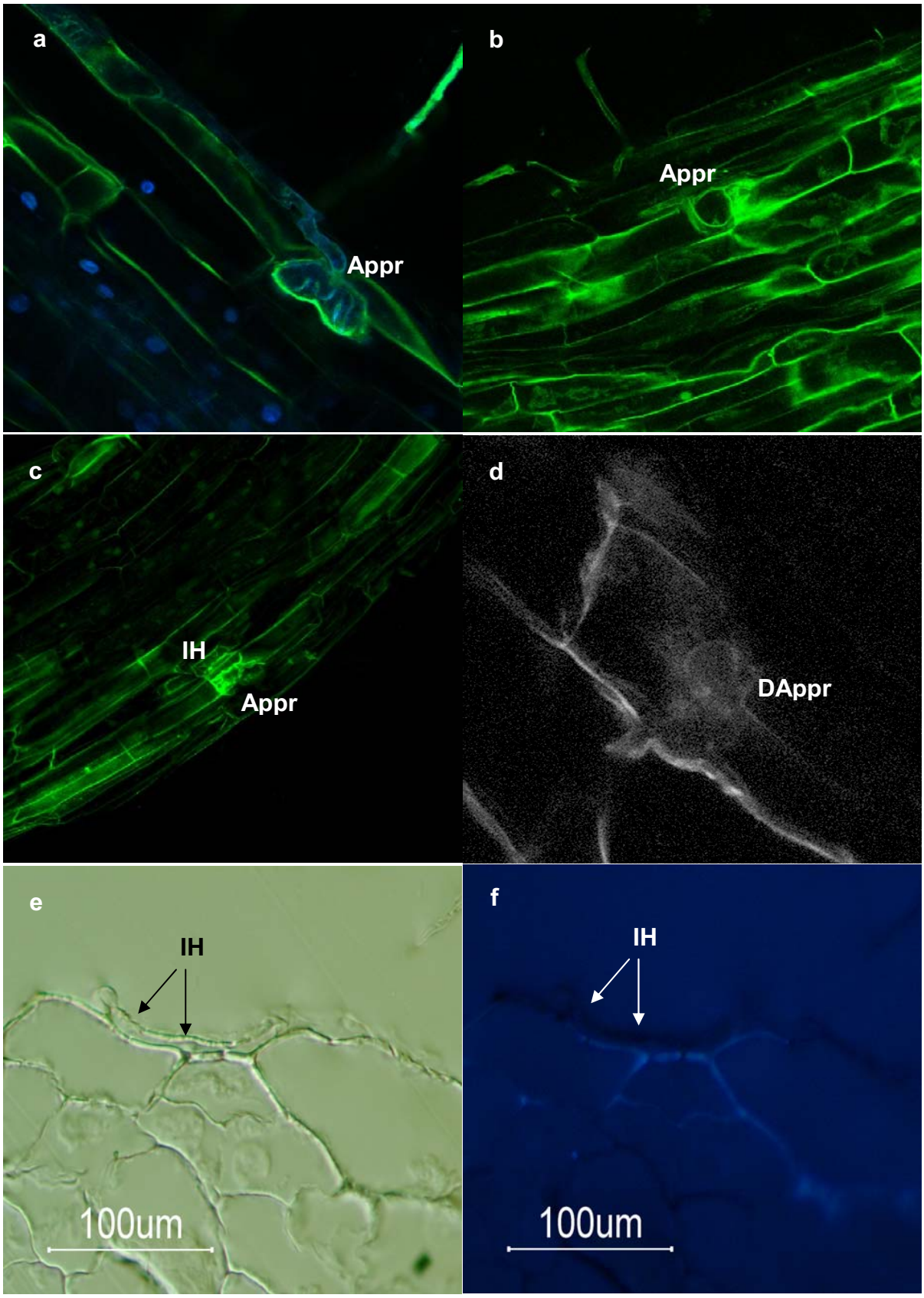
a
Appr
b
Appr
c
IH
Appr
d
DAppr
e
IH
100um
f
IH
100um

5.4. Discussion

To comprehend better the results obtained in this Chapter, they are summarized in Table 5.3. Wild-type tomato roots were readily colonized by the three different AM fungi leading to the formation of arbuscules 3-5 days after being transplanted into the nurse pots. Generally, fungal colonization followed similar steps to form arbuscules or arbusculate coils in the cortical cells. Most of the fungal structures were active and induced the movement of the plant nuclei to a central position as shown before by Ballestrini *et al*. (1992) and Cavagnaro *et al.* (2001b) working with *Arum*-type and *Paris*-type AM, respectively. AM fungal colonization induced autofluorescence at the penetration sites of the wild-type, as well as at the points where hyphae were growing from the exodermal cells to the cortex to colonize new cells. Autofluorescence was not observed in cells containing completely formed arbuscules. However, the autofluorescence was not associated with callose deposits. Autofluorescence at the site of penetration has been described before for incompatible pathogen-plant interactions (Bennett *et al.*, 1996) as an indication of plant defense reaction. However, in the case of AM interactions only weak autofluorescence under blue light has been found (Cordier *et al.*, 1996; Garriock *et al.*, 1989), as proof that phenolic compounds do not accumulate. Nevertheless, the responses to AM penetration are diverse and can also include accumulation of hydroxyproline-rich glycoprotein (HRGP), although the role of this compound in plant defense in AM interactions has not been confirmed (Balestrini *et al.*, 1994). Another possibility to explain the presence of this autofluorescence, is the production of wall-degrading enzymes such as pectinase and cellulase by AM fungi (Garcia-Romera *et al.*, 1991) which could cause controlled damage to the root cells. Deposits of callose were very small with all the inoculated fungi, as has been shown before with different plant-fungus interactions (Balestrini *et al.*, 1994; Bonfante *et al.*, 2000).

Table 5.3. Cellular responses in wild-type and *rmc* tomato to AM fungi forming different colonization phenotypes. (-) to (++) indicates negative to strong response. * Internal hyphae (IH) in this case do not include cortical colonization. # Position of the plant nuclei after penetration of the AM fungi, independent of the type of cell: exodermis or cortex. Labels are; *Intra*, *G*. *intraradices*; *calospora*, *S*. *calospora.*

Cellular responses	**Pen-**, *intra* BEG159	**Coi-**, *calospora* WUM 12(2)	**Myc+**, *intra* VFVAM23
Active Appr			
wild-type	++	++	++
rmc	±	±	±
Active IH*			
wild-type	++	++	++
rmc	_	±	++
Active Arb			
wild-type	++	++	++
rmc	_	_	++
Autofluorescence Appr			
wild-type	++	NA	++
rmc	++	NA	++
Autofluorescence IH*			
wild-type	+	+	+
rmc	NA	+	+
Autofluorescence Arb			
wild-type	_	_	_
rmc	NA	NA	_
Callose deposition			
wild-type	±	±	±
rmc	_	_	_
Position of plant nuclei#			
wild-type	Central	Central	Central
rmc	Periphery	± Central then periphery	Central

Although AM colonization in *rmc* is restricted in the Pen- and Coi- phenotypes, appressorium formation was not blocked at the epidermis. This is in accordance with the majority of AM mutants described so far (see Table 2.1 for details) because all AM fungi challenged against *rmc* have formed appressoria (see also chapter 7). This finding differs from non-host plants, in which fungal growth and appressorium formation are not supported (Giovannetti *et al.*, 1993; Glenn *et al.*, 1988). Another important finding is that the appressoria were as active as with the wild-type when they established first contact with *rmc*, as demonstrated with NBT/AF method. This indicates that the signal for appressorium development might rest at the epidermis, as suggested before by Tester *et al.* (1987) and discussed further by Bonfante *et al.* (2000) and Novero *et al.* (2002), who gave not only morphological evidence but also genetic data that the allele *Ljsym*4-1 is necessary to overcome AM blockage at the epidermis in the *L. japonicus* mutant EMS 1749.

Fungi developing the Pen- phenotype did not penetrate the epidermal cells and there was no change in the position of plant nuclei or deposition of callose. This phenotype showed no significant accumulation of defense-related gene mRNAs either (Gao *et al.*, 2004), reaffirming the idea that products of plant defense-related genes do not restrict AM fungal development (Harrison & Dixon, 1993). Furthermore, the induction of autofluorescence that was observed may be related to cell death or plant membrane damage because callose was not detected using aniline blue stain. This result differs from observations with other mutants such as the P2 mutant of pea (Gollotte *et al.*, 1993) in which callose was responsible for blocking the AM fungal penetration. In the Coi- phenotype with *S. calospora* the development of IH in the exodermis alone was enough to cause movement of nuclei to a central position, although the change in the position was temporary due to the blockage at this stage and subsequent death of the IH. Callose deposits were not observed, consistent with the idea that this compound is not responsible for the

blockage. This phenotype showed strong and sustained expression of defense-related genes in the study by Gao *et al*. (2004). The authors suggested that the response may be related to the degree of penetration of the exodermis. Penetration by AM fungus requires the activation of an intracellular accommodation apparatus (pre-penetration apparatus, PPA) that is likely to be responsible for the synthesis of the compartment required for hyphal containment that precedes successful colonization. Furthermore, the *Medicago truncatula* infection-related *ENOD11* gene was always expressed in cells forming the PPA. Neither PPA formation nor *ENOD11* expression were observed in the *dmi2-2* and *dmi3-1* mutants, which do not support fungal penetration. In addition, in *L. japonicus*, the allele *Ljsym4-1* is required for the accommodation process to support AM fungal development which also includes the deposition of wall material around the fungus (Bonfante *et al.*, 2000). This cell wall material deposited continually around the fungus did not contain callose or phenolics compounds (Lemoine *et al.*, 1995).

The Myc+ phenotype with *G*. *intraradices* WFVAM23 seems to be a normal mycorrhiza very similar to the wild-type, except that the percentage of arbuscules was always lower. The formation of typical *Arum*-type arbuscules was associated with movement of the cortical cell nuclei of *rmc* to a central position, as in the wild-type. Normal arbuscules have been observed before in other mutants such as the *Ljsym4-1* and *Ljsym4-2 L. japonicus* mutants. However activity and morphology of these arbuscules were not assessed. In Table 5.2 it can be observed that arbuscules in this phenotype were always active and in Chapter 3, I demonstrated that they transfer enough C to allow *rmc* to produce small spores. In addition Gao *et al*. (2004) found that this phenotype did not show an increase in the levels of transcripts related to plant defense when compared with the *Arum*-type mycorrhiza of the wild-type. These results indicate that the fungus is able to overcome the block in *rmc* that restricts colonization by other fungi. This adds another confirmation of

the diversity in functional responses of AM. The fact that *rmc* is able to form different phenotypes and that the cellular responses are different (Table 5.3) indicate that mycorrhiza formation is controlled by multiple mechanisms as suggested before (Novero *et al.*, 2002).